THE JOURNAL OF BIOLOGICAL CHEMISTRY VOL. 289, NO. 20, pp. 14157–14169, May 16, 2014


# The Association of Cortactin with Profilin-1 Is Critical for Smooth Muscle Contraction*

Received for publication, January 6, 2014, and in revised form, March 27, 2014 Published, JBC Papers in Press, April 3, 2014, DOI 10.1074/jbc.M114.548099

**Ruping Wang, Rachel A. Cleary, Tao Wang, Jia Li, and Dale D. Tang**[1]

*From the Center for Cardiovascular Sciences, Albany Medical College, Albany, New York 12208*

**Background:** Profilin-1 (Pfn-1) regulates actin dynamics and contraction in smooth muscle.
**Results:** Contractile activation increases the association of cortactin with Pfn-1 via c-Abl, which controls actin dynamics and contraction.
**Conclusion:** The coupling of cortactin with Pfn-1 regulated by c-Abl is critical for actin polymerization and contraction.
**Significance:** The c-Abl-mediated cortactin/Pfn-1 interaction is a novel mechanism for the regulation of smooth muscle contraction.

**Profilin-1 (Pfn-1) is an actin-regulatory protein that has a role in modulating smooth muscle contraction. However, the mechanisms that regulate Pfn-1 in smooth muscle are not fully understood. Here, stimulation with acetylcholine induced an increase in the association of the adapter protein cortactin with Pfn-1 in smooth muscle cells/tissues. Furthermore, disruption of the protein/protein interaction by a cell-permeable peptide (CTTN-I peptide) attenuated actin polymerization and smooth muscle contraction without affecting myosin light chain phosphorylation at Ser-19. Knockdown of cortactin by lentivirus-mediated RNAi also diminished actin polymerization and smooth muscle force development. However, cortactin knockdown did not affect myosin activation. In addition, cortactin phosphorylation has been implicated in nonmuscle cell migration. In this study, acetylcholine stimulation induced cortactin phosphorylation at Tyr-421 in smooth muscle cells. Phenylalanine substitution at this position impaired cortactin/Pfn-1 interaction in response to contractile activation. c-Abl is a tyrosine kinase that is necessary for actin dynamics and contraction in smooth muscle. Here, c-Abl silencing inhibited the agonist-induced cortactin phosphorylation and the association of cortactin with Pfn-1. Finally, treatment with CTTN-I peptide reduced airway resistance and smooth muscle hyperreactivity in a murine model of asthma. These results suggest that the interaction of cortactin with Pfn-1 plays a pivotal role in regulating actin dynamics, smooth muscle contraction, and airway hyperresponsiveness in asthma. The association of cortactin with Pfn-1 is regulated by c-Abl-mediated cortactin phosphorylation.**

Smooth muscle contraction is essential for the regulation of bodily functions including the maintenance of appropriate airway tone and blood pressure. Abnormal smooth muscle contraction contributes to the pathogenesis of smooth muscle diseases such as asthma and hypertension.

Contractile activation induces myosin light chain phosphorylation at Ser-19, which activates myosin ATPase and initiates sliding of contractile filaments and smooth muscle contraction (1–3). In addition, contractile stimulation induces actin filament polymerization, which may promote contraction by enhancing transmission of force between contractile units and extracellular matrix and by increasing contractile units (4–8). Thus, both myosin light chain phosphorylation and actin cytoskeletal reorganization are required for contraction of smooth muscle. Although myosin activation has been extensively studied (1–3), the mechanisms that regulate actin polymerization are not fully understood.

Profilin-1 (Pfn-1)[2] is an actin-binding protein that is ubiquitously expressed in mammalian cells (7, 9). Pfn-1 has been implicated in promoting actin polymerization *in vitro* (9) and migration/proliferation of nonmuscle cells (10). Pfn-1 promotes actin polymerization by catalyzing the exchange of actin-bound ADP for ATP and by releasing actin monomer from thymosin-$\beta$4; both processes facilitate unidirectional addition of G-actin to F-actin (7, 8, 11). In smooth muscle, down-regulation of Pfn-1 inhibits actin polymerization and contractile force without affecting myosin light chain phosphorylation (12). The mechanisms that regulate Pfn-1 activation are not well elucidated.

Cortactin is an adapter protein that is able to regulate actin filament assembly and branching in *in vitro* studies as well as adhesion, migration, and endocytosis of nonmuscle cells (13, 14). Cortactin undergoes phosphorylation on Tyr-421 in fibroblasts during cell migration, and this has been implicated in the activation of cortactin (14). Cortactin may regulate actin polymerization by affecting the functional state of neuronal Wiskott-Aldrich syndrome protein, the Arp2/3 complex, and Nck in nonmuscle cells such as mouse embryonic fibroblasts and mouse 3T3 cells (13, 15). However, the interaction of cortactin with Pfn-1 has not been explored.

c-Abl (Abelson tyrosine kinase, Abl) is a non-receptor tyrosine kinase that has a role in the regulation of actin dynamics,

* This work was supported, in whole or in part, by National Institutes of Health Grants HL-110951 and HL-113208 (to D. D. T.).
[1] To whom correspondence should be addressed: Center for Cardiovascular Sciences, Albany Medical College, 47 New Scotland Ave., MC-8, Albany, NY 12208. Tel.: 518-262-6416; Fax: 518-262-8101; E-mail: tangd@mail.amc.edu.

[2] The abbreviations used are: Pfn-1, profilin-1; ACh, acetylcholine; c-Abl, Abelson tyrosine kinase; HASM, human airway smooth muscle; KD, knockdown; OVA, ovalbumin.

cell adhesion, migration, proliferation, growth, and development (16–19). Recent studies have implicated c-Abl in the regulation of smooth muscle contraction. Contractile activation induces c-Abl phosphorylation, an indication of c-Abl activation (20, 21), in smooth muscle. Knockdown of c-Abl attenuates smooth muscle force development in response to contractile activation (21–23). The role of c-Abl in regulating Pfn-1 has not been investigated.

The objective of this study was to assess whether the interaction of cortactin with Pfn-1 is necessary for smooth muscle contraction. Moreover, we evaluated the potential role of c-Abl in regulating the coupling of cortactin with Pfn-1.

## EXPERIMENTAL PROCEDURES

*Cell Culture*—Human airway smooth muscle (HASM) cells were prepared from human bronchi and adjacent tracheas obtained from the International Institute for Advanced Medicine (16). Human tissues were non-transplantable and consented for research. This study was approved by the Albany Medical College Committee on Research Involving Human Subjects. Briefly, muscle tissues were incubated for 20 min with dissociation solution (130 mM NaCl, 5 mM KCl, 1.0 mM $CaCl_2$, 1.0 mM $MgCl_2$, 10 mM Hepes, 0.25 mM EDTA, 10 mM D-glucose, 10 mM taurine, pH 7, 4.5 mg of collagenase (type I), 10 mg of papain (type IV), 1 mg/ml BSA, and 1 mM dithiothreitol). All enzymes were purchased from Sigma-Aldrich. The tissues were then washed with Hepes-buffered saline solution (composed of 10 mM Hepes, 130 mM NaCl, 5 mM KCl, 10 mM glucose, 1 mM $CaCl_2$, 1 mM $MgCl_2$, 0.25 mM EDTA, and 10 mM taurine, pH 7). The cell suspension was mixed with Ham's F-12 medium supplemented with 10% (v/v) fetal bovine serum (FBS) and antibiotics (100 units/ml penicillin and 100 $\mu$g/ml streptomycin). Cells were cultured at 37 °C in the presence of 5% $CO_2$ in the same medium. The medium was changed every 3–4 days until cells reached confluence, and confluent cells were passaged with trypsin/EDTA solution (16, 24, 25). Smooth muscle cells within passage 5 were used for the studies.

*Immunoblot Analysis*—Cells were lysed in SDS sample buffer composed of 1.5% dithiothreitol, 2% SDS, 80 mM Tris-HCl, pH 6.8, 10% glycerol, and 0.01% bromphenol blue. The lysates were boiled in the buffer for 5 min and separated by SDS-PAGE. Proteins were transferred to a nitrocellulose membrane. The membrane was blocked with bovine serum albumin or milk for 1 h and probed using primary antibody followed by horseradish peroxidase-conjugated secondary antibody (Fisher Scientific). Proteins were visualized by enhanced chemiluminescence (Fisher Scientific) using the Fuji LAS-4000 imaging system. Antibodies against cortactin, phosphocortactin (Tyr-421), phospho-myosin light chain (Ser-19), myosin light chain, and Pfn-1 were purchased from Santa Cruz Biotechnology and Cell Signaling Technology. c-Abl antibody was purchased from BD Biosciences and Santa Cruz Biotechnology. Glyceraldehyde-3-phosphate dehydrogenase (GAPDH) antibody was purchased from Fitzgerald (Acton, MA). The levels of total protein or phosphoprotein were quantified by scanning densitometry of immunoblots (Fuji MultiGauge software). The luminescence signals from all immunoblots were within the linear range.

*Co-immunoprecipitation Analysis*—Co-immunoprecipitation analysis was used to evaluate protein/protein interactions as described previously (23, 25). Briefly, cell/tissue extracts were incubated overnight with corresponding antibodies and then incubated for 2–3 h with 125 $\mu$l of a 10% suspension of protein A-Sepharose beads. Immunocomplexes were washed four times in buffer containing 50 mM Tris-HCl, pH 7.6, 150 mM NaCl, and 0.1% Triton X-100. The immunoprecipitates were separated by SDS-PAGE followed by transfer to nitrocellulose membranes. The membranes of immunoprecipitates were probed using corresponding antibodies.

*Immunofluorescence and Fluorescence Analysis*—Cells in dishes containing coverslips were fixed for 15 min in 4% paraformaldehyde and then washed three times in phosphate-buffered saline (PBS) followed by permeabilization with 0.2% Triton X-100 dissolved in PBS for 5 min. These cells were immunofluorescently stained using specific antibodies followed by appropriate secondary antibodies (Invitrogen). The cellular localization of fluorescently labeled proteins was viewed under a high resolution digital fluorescence microscope (Leica; 63× oil objective). The localization of labeled protein was also line-scanned using Leica image software. The time of image capturing, intensity gaining, and image contrast in both channels were optimally adjusted and kept constant for all experiments to standardize the fluorescence intensity measurements among experiments. For quantification analysis, cells with >50% of periphery displaying colocalized proteins were considered colocalized cells. The percentage of cells with colocalization was calculated as follows: (Number of cells with colocalization/Number of total cells observed) × 100.

*Preparation of a Cell-permeable Decoy Peptide*—A cell-permeable decoy peptide (CTTN-I) was designed to disrupt the interaction of cortactin with Pfn-1. The sequence of CTTN-I peptide was taken from the Pro-rich domain of cortactin (sequence is TEERLPSSPVYEDAASFKAE) (NCBI accession number NM_005231). This peptide is able to compete with endogenous cortactin for Pfn-1 binding (26). The N-terminal end of the peptide was fused with trans-activator of transcription (TAT) sequence (GRKKRRQRRRPPQ) for cell permeability. Trans-activator of transcription peptide is a short polybasic sequence derived from the HIV trans-activator of transcription protein; it has been shown to successfully deliver a large variety of cargos (from small particles to peptides and proteins) into intact cells/tissues (27). The peptide was synthesized and purified by Invitrogen. A peptide with scrambled sequence (EPSETSVEYDEARALSKAPF) was also used as a control.

*Virus-mediated RNAi and Gene Expression*—For cortactin knockdown (KD), lentiviruses encoding cortactin shRNA or control shRNA were purchased from Santa Cruz Biotechnology. HASM cells were infected with control shRNA lentivirus or cortactin shRNA lentivirus for 12 h. They were then cultured for 3–4 days. Positive clones expressing shRNAs were selected by puromycin. Immunoblot analysis was used to determine the expression levels of cortactin in these cells. Cortactin KD cells and cells expressing control shRNA were stable at least five passages after initial infection. The experimental procedures for generating c-Abl KD cells were described previously (16, 17).

To assess the role of cortactin phosphorylation, wild type cortactin (28) was used to generate cortactin Y421F (phenylalanine substitution at Tyr-421). The constructs were inserted into retrovirus vectors as described previously (28). Retrovirus production and cell infection were performed using a method described previously (16, 24, 29).

*In Vitro Protein Binding Assay*—*In vitro* protein/protein interaction was assessed using the method described previously (15, 16, 30). Purified cortactin was covalently coupled to Affi-Gel 15 resin (Bio-Rad) according to the manufacturer's protocol. The cortactin beads were washed twice with ice-cold binding buffer (50 mM Hepes, pH 7.25, 125 mM NaCl, 0.01% Nonidet P-40, and 5% glycerol) and stored as a 50% slurry. Different concentrations of Pfn-1 (Cytoskeleton) were added to tubes containing cortactin bead slurry or blank bead slurry blocked with an excess of ethanolamine. The reaction was incubated at 4 °C for 2 h. The supernatant was removed, and the beads were rapidly resuspended in ice-cold binding buffer. Bound material was recovered with 5× SDS sample buffer, separated by SDS-PAGE, stained with Coomassie Blue R-250, and scanned using the Fuji imaging system. Binding curves were generated using the equation $Y = (B_{max} \times X)/(X + K_d) + NS \times X$ where $Y$ equals the specific binding signal, $X$ equals the concentration of ligand added to the cortactin beads, and NS equals the slope of the least square linear regression fit for the nonspecific binding as measured with the blank beads. Recombinant cortactin was generated using the methods described previously (15, 24, 25). Profilin-1 was purchased from Cytoskeleton. Site-directed mutagenesis was performed using the Stratagene QuikChange mutagenesis kit.

*In Vitro Kinase Assay*—Cortactin was produced using methods described previously (15, 24, 25, 31). Cortactin and c-Abl (100 ng; Invitrogen) were placed in kinase buffer containing 10 mM Hepes, pH 7.4, 3 mM $MnCl_2$, and 2 mM DTT. The kinase reaction was initiated by the addition of 20 $\mu$M ATP at 30 °C (with shaking) for 30 min and stopped by the addition of SDS sample buffer. The reaction mixture was separated by SDS-PAGE followed by membrane transfer. The membrane was probed with phosphocortactin antibody (Tyr-421), stripped, and reprobed with cortactin antibody.

*Analysis of F-actin/G-actin Ratios*—The content of F-actin and G-actin in smooth muscle was measured using a method described previously (23, 32, 33). Briefly, smooth muscle cells were treated with F-actin stabilization buffer (50 mM PIPES, pH 6.9, 50 mM NaCl, 5 mM $MgCl_2$, 5 mM EGTA, 5% glycerol, 0.1% Triton X-100, 0.1% Nonidet P40, 0.1% Tween 20, 0.1% $\beta$-mercaptoethanol, 1 mM ATP, 1 $\mu$g/ml pepstatin, 1 $\mu$g/ml leupeptin, and 10 $\mu$g/ml benzamidine). The supernatants of protein extracts were collected after centrifugation at 151,000 × *g* for 60 min at 37 °C. The pellets were resuspended in ice-cold $H_2O$ plus 1 $\mu$M cytochalasin D and then incubated on ice for 1 h to dissociate F-actin. The resuspended pellets were gently mixed every 15 min. The supernatant of the resuspended pellets was collected after centrifugation at 16,100 × *g* for 2 min at 4 °C. An equal volume of the first supernatant (G-actin) or second supernatant (F-actin) was subjected to immunoblot analysis using $\alpha$-actin antibody. The amount of F-actin and G-actin was determined by scanning densitometry.

*Assessment of Tracheal Ring Contraction*—Mice were euthanized by injection of pentobarbital (140 mg/kg). All experimental protocols were approved by the Institutional Animal Care and Usage Committee. A segment of trachea (4–5 mm in length) was immediately removed and placed in physiological saline solution containing 110 mM NaCl, 3.4 mM KCl, 2.4 mM $CaCl_2$, 0.8 mM $MgSO_4$, 25.8 mM $NaHCO_3$, 1.2 mM $KH_2PO_4$, and 5.6 mM glucose. The solution was aerated with 95% $O_2$ and 5% $CO_2$ to maintain a pH of 7.4. Two stainless steel wires were passed through the lumen of tracheal rings. One of the wires was connected to the bottom of organ baths, and the other was attached to a Grass force transducer that had been connected to a computer with analog/digital converter (Grass). Tracheal segments were then placed in physiological saline solution at 37 °C. Passive tension with 0.5 g was applied to each segment for 20–30 min. Contractile force in response to various treatments was then measured.

*Measurement of Human Bronchial Ring Contraction*—Bronchial rings (diameter, 5 mm) were prepared from human lungs obtained from the International Institutes for Advanced Medicine (see above). Bronchial rings were placed in physiological saline solution at 37 °C in a 25-ml organ bath and attached to a Grass force transducer that had been connected to a computer with analog/digital converter (Grass). For lentivirus-mediated RNAi in tissues, the epithelium layer of human bronchial rings was removed by using forceps. Bronchial rings were then transduced with lentivirus encoding cortactin shRNA or control shRNA for 3 days. Force development in response to acetylcholine (ACh) (100 $\mu$M; 10 min) activation was compared before and after lentivirus transduction. For biochemical analysis, human tissues were frozen using liquid nitrogen and pulverized as described previously (30, 34, 35).

*Animals and Measurement of Airway Resistance*—To assess the effects of peptides, BALB/c mice (6–7 weeks old) were purchased from The Jackson Laboratory. Mice were sensitized by intraperitoneal injection of sterile LPS-free ovalbumin (OVA) (Pierce) or PBS (control) weekly for 3 weeks and challenged with intranasal instillations of OVA or PBS (control) twice a week for 8 weeks using protocols described previously (36, 37) with minor modifications. In addition, animals were intranasally instilled with 1 mg/kg peptides 0.5 h before OVA instillation and 5.5 h after OVA instillation for the last 3 weeks. Airway resistance in these mice was then assessed on Day 77.

To measure airway resistance, mice were anesthetized with an intraperitoneal injection of pentobarbital sodium, tracheotomized, and connected to the FlexiVent system (SCIREQ Inc., Montreal, Canada). Mice were mechanically ventilated at 150 breaths/min with a tidal volume of 10 ml/kg and a positive end expiratory pressure of 3.35 cm $H_2O$. Following baseline measurements, mice were challenged with methacholine aerosol for 10 s at different doses. Airway resistance was measured for each mouse after inhalation of the aerosol. A dose-response curve was then determined. This study was approved by the Institutional Committee of Animal Care and Usage of Albany Medical College.

*Statistical Analysis*—All statistical analysis was performed using Prism 6 software (GraphPad Software, San Diego, CA). Comparison among multiple groups was performed by one-

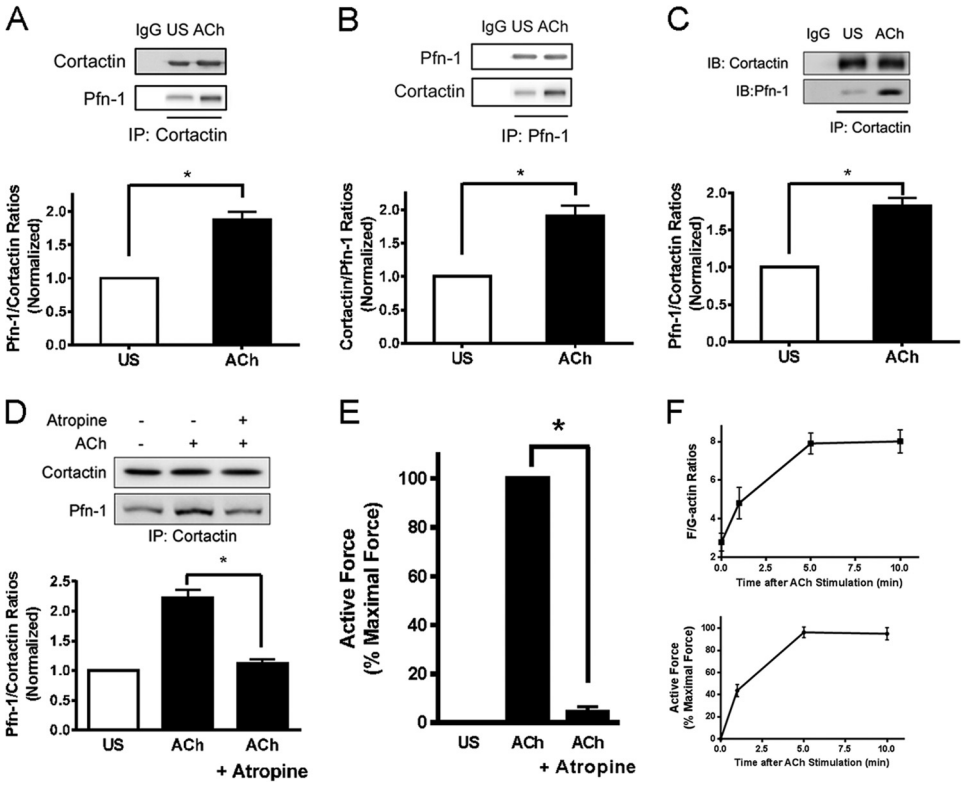


FIGURE 1. **Contractile activation increases the association of cortactin with Pfn-1 in smooth muscle cells/tissues.** *A*, cortactin immunoprecipitates of HASM cells that had been treated with ACh (100 $\mu$M; 5 min) or left unstimulated (*US*) were separated by SDS-PAGE and blotted with antibodies against cortactin and Pfn-1. Cortactin antibody, but not IgG, immunoprecipitates cortactin and Pfn-1. The ratios of Pfn-1 over cortactin are significantly higher in stimulated cells than in unstimulated cells (*, $p < 0.05$). Data are mean values of four independent experiments. *Error bars* indicate S.E. *B*, blots of Pfn-1 immunoprecipitates from HASM cells treated with or without ACh (100 $\mu$M; 5 min) were blotted with antibodies against cortactin and Pfn-1. Pfn-1 antibody, but not IgG, immunoprecipitates cortactin and Pfn-1. The ratios of cortactin/Pfn-1 are significantly higher in stimulated cells than in unstimulated cells (*, $p < 0.05$). Data are mean values of four independent experiments. *Error bars* indicate S.E. *C*, extracts of human bronchial rings treated with or without ACh were precipitated with cortactin antibody and blotted with antibodies against cortactin and Pfn-1. The Pfn-1/cortactin ratios are significantly higher in stimulated tissues than in unstimulated tissues (*, $p < 0.05$; $n = 3$). *D*, pretreatment with atropine (1 $\mu$M; 10 min) inhibits the association of cortactin with Pfn-1 induced by ACh (100 $\mu$M; 5 min) (*, $p < 0.05$; $n = 4$). *E*, pretreatment with atropine (1 $\mu$M; 10 min) inhibits contraction in human bronchial tissues induced by ACh (100 $\mu$M; 5 min) (*, $p < 0.05$; $n = 4$). *F*, *top panel*, time dependence of F/G-actin ratios in HASM cells in response to ACh stimulation. F/G-actin ratios were determined by the fractionation assay ($n = 3$). *Bottom panel*, force development in human bronchial rings during ACh stimulation was determined using a muscle research system ($n = 3$). Force is expressed as the percentage of maximal response to 100 $\mu$M ACh. *IP*, immunoprecipitation; *IB*, immunoblot.

way analysis of variance followed by Tukey's multiple comparison test. Differences between pairs of groups were analyzed by Student-Newman-Keuls test or Dunn's method. Values of *n* refer to the number of experiments used to obtain each value. $p < 0.05$ was considered to be significant.

## RESULTS

*Interaction of Cortactin with Pfn-1 Is Enhanced in Smooth Muscle during ACh Stimulation*—As described above, Pfn-1 is able to regulate actin dynamics and smooth muscle contraction. The upstream regulator of Pfn-1 is not well identified. Because cortactin has been implicated in actin cytoskeletal remodeling (13, 14), we hypothesized that contractile stimulation may promote the association of cortactin with Pfn-1, which may activate Pfn-1 in smooth muscle in response to contractile activation. To test this, HASM cells were stimulated with ACh (a stimulus implicated in airway tone and asthma) (38) for 5 min, or cells were unstimulated. Cell extracts were immunoprecipitated using cortactin antibody and blotted with antibodies against cortactin and Pfn-1. The amount of Pfn-1 in cortactin immunoprecipitates was higher in stimulated cells than in unstimulated cells. The ratios of Pfn-1/cortactin were increased in stimulated cells compared with unstimulated cells (Fig. 1*A*).

To verify this, we used reverse co-immunoprecipitation analysis. Cell extracts were immunoprecipitated using Pfn-1 antibody, and blots of the immunoprecipitates were probed using antibodies against cortactin and Pfn-1. The ratios of cortactin over Pfn-1 in stimulated cells were higher as compared with unstimulated cells (Fig. 1*B*).

Furthermore, we evaluated the effects of contractile activation on the interaction of cortactin with Pfn-1 at the tissue level. Human bronchial rings were treated with ACh, and cortactin immunoprecipitates of tissue extracts were subjected to immunoblot analysis. The level of Pfn-1 in cortactin precipitates was higher in stimulated tissues than in unstimulated tissues (Fig. 1*C*).

We also evaluated the effects of the muscarinic receptor antagonist atropine on the association of Pfn-1 with cortactin. Treatment with atropine reduced the increase in Pfn-1/cortactin ratios and contraction (Fig. 1, *D* and *E*). The results suggest that the ACh-induced increase in Pfn-1/cortactin interaction is mediated by muscarinic receptor. Moreover, ACh stimulation

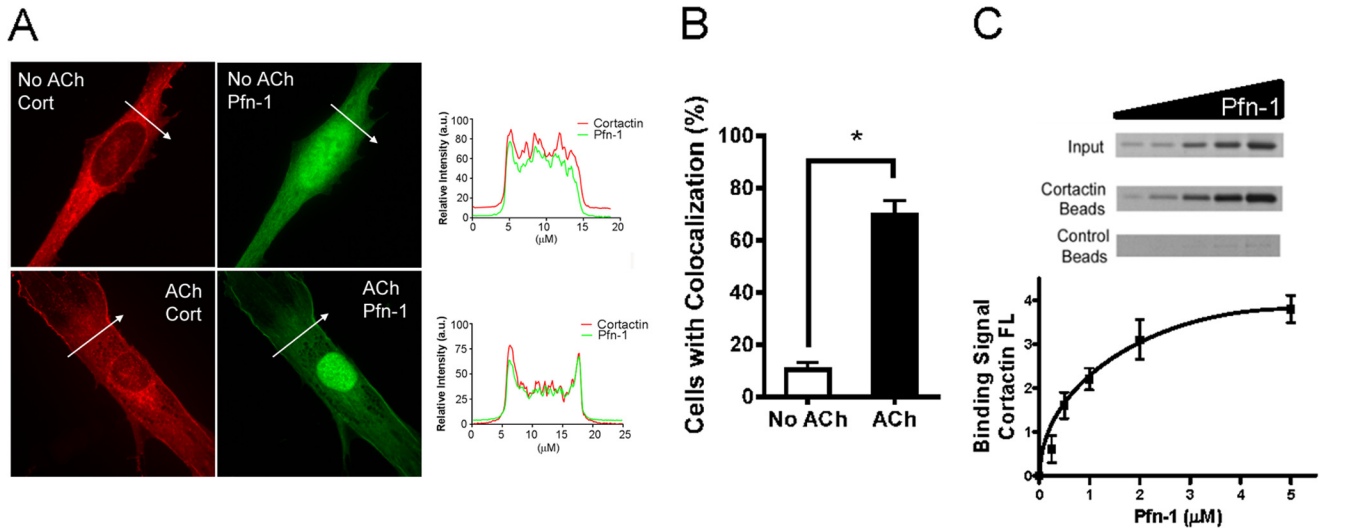


FIGURE 2. **Cortactin and Pfn-1 undergo spatial redistribution in smooth muscle cells upon contractile activation.** *A*, HASM cells were stimulated with ACh (100 $\mu$M; 5 min) or left unstimulated. The cellular localization of cortactin and Pfn-1 was evaluated by immunofluorescence microscopy. Representative images illustrate the spatial redistribution of cortactin and Pfn-1 in response to ACh activation. *Arrows* indicate a single line scan to analyze the fluorescence signal for each cell. *Cort*, cortactin. The line scan graphs show co-localization and relative fluorescence intensity of the two proteins. *B*, the percentage of cells with colocalization was calculated as follows: (Number of cells with colocalization/Number of total cells observed) $\times$ 100. *, significantly higher cell numbers after stimulation with ACh compared with unstimulated cells ($p < 0.05$). Data are mean values of three independent experiments. *Error bars* indicate S.E. *C*, representative gel images illustrating the binding of Pfn-1 to cortactin beads but not to control beads. Binding of Pfn-1 to cortactin is concentration-dependent ($n = 3$). *a.u.*, arbitrary units; *FL*, fluorescence.

induced coordinate increases in F/G-actin ratios and contraction in HASM cells/tissues (Fig. 1*F*).

We also used immunofluorescence microscopy to assess the spatial localization of Pfn-1 and cortactin in response to contractile activation. In unstimulated cells, Pfn-1 was localized in the cytoplasm and the nucleus of smooth muscle cells. Upon ACh stimulation, Pfn-1 translocated to the cell periphery (Fig. 2, *A* and *B*). Furthermore, cortactin was localized in the cytoplasm of unstimulated cells. Cortactin was colocalized with Pfn-1 in the cortical region of cells in response to ACh activation (Fig. 2, *A* and *B*).

We used an affinity pulldown assay to determine whether cortactin directly binds to Pfn-1. The same amount of cortactin beads was incubated with different concentration of Pfn-1. After reaching equilibrium, the amount of cortactin-bound Pfn-1 was evaluated. Pfn-1 binds to cortactin in a concentration-dependent manner (Fig. 2*C*).

*Interaction of Cortactin with Pfn-1 Is Inhibited by CTTN-I Peptide*—To assess the importance of cortactin/Pfn-1 coupling in cells, we used CTTN-I peptide, a cell-permeable peptide, to disrupt the protein/protein interaction. The sequence of this peptide contains Tyr-421 and adjacent residues, which are able to compete with endogenous cortactin for Pfn-1 binding (26, 39). We used co-immunoprecipitation analysis to evaluate the effects of CTTN-I peptide on the protein/protein interaction. The amount of Pfn-1 co-immunoprecipitated with cortactin during ACh stimulation was lower in cells treated with CTTN-I peptide than in cells treated with scrambled (control) peptide (Fig. 3*A*). Moreover, colocalization of Pfn-1 with cortactin on the edge in response to ACh activation was reduced in cells treated with CTTN-I peptide compared with cells treated with control peptide (Fig. 3, *B* and *C*). However, cortactin phosphorylation during ACh stimulation was not affected by CTTN-I peptide (Fig. 3*D*). The results suggest that CTTN-I peptide selectively impairs the coupling of cortactin with Pfn-1.

*Disruption of Cortactin/Pfn-1 Coupling by CTTN-I Peptide Inhibits Contraction and Actin Polymerization without Affecting Myosin Phosphorylation*—To determine the functional role of cortactin/Pfn-1 coupling, HASM cells were treated with peptides followed by contractile activation. F/G-actin ratios in these cells were then determined. F/G-actin ratios upon contractile activation were reduced in cells treated with CTTN-I peptide compared with cells treated with control peptide (Fig. 4*A*). Furthermore, we also determined the effects of CTTN-I peptide on smooth muscle contraction. Contractile force was attenuated in human bronchial rings and mouse tracheal rings treated with CTTN-I peptide (Fig. 4, *B* and *C*). However, myosin light chain phosphorylation was not affected by CTTN-I peptide (Fig. 4*D*).

*Cortactin Is Required for Smooth Muscle Contraction and Actin Polymerization but Not Myosin Phosphorylation*—Cortactin has been implicated in adhesion, migration, and endocytosis of nonmuscle cells (13, 14). The role of cortactin in smooth muscle contraction has not been investigated. To determine the role of cortactin, we utilized a lentivirus-mediated RNAi approach (35) to inhibit the expression of cortactin. The contractile response of human bronchial rings to ACh was evaluated. Bronchial rings were then transduced with lentiviruses encoding control shRNA or cortactin shRNA. These tissues were incubated in the medium for 3 days. Contractile force of these tissues was then evaluated. Immunoblot analysis verified the lower expression of cortactin in tissues transduced with viruses encoding cortactin shRNA compared with uninfected rings and tissues transduced with viruses for control shRNA (Fig. 5*A*). More importantly, contractile responses of human bronchial rings were lower in cortactin-deficient tissues than in

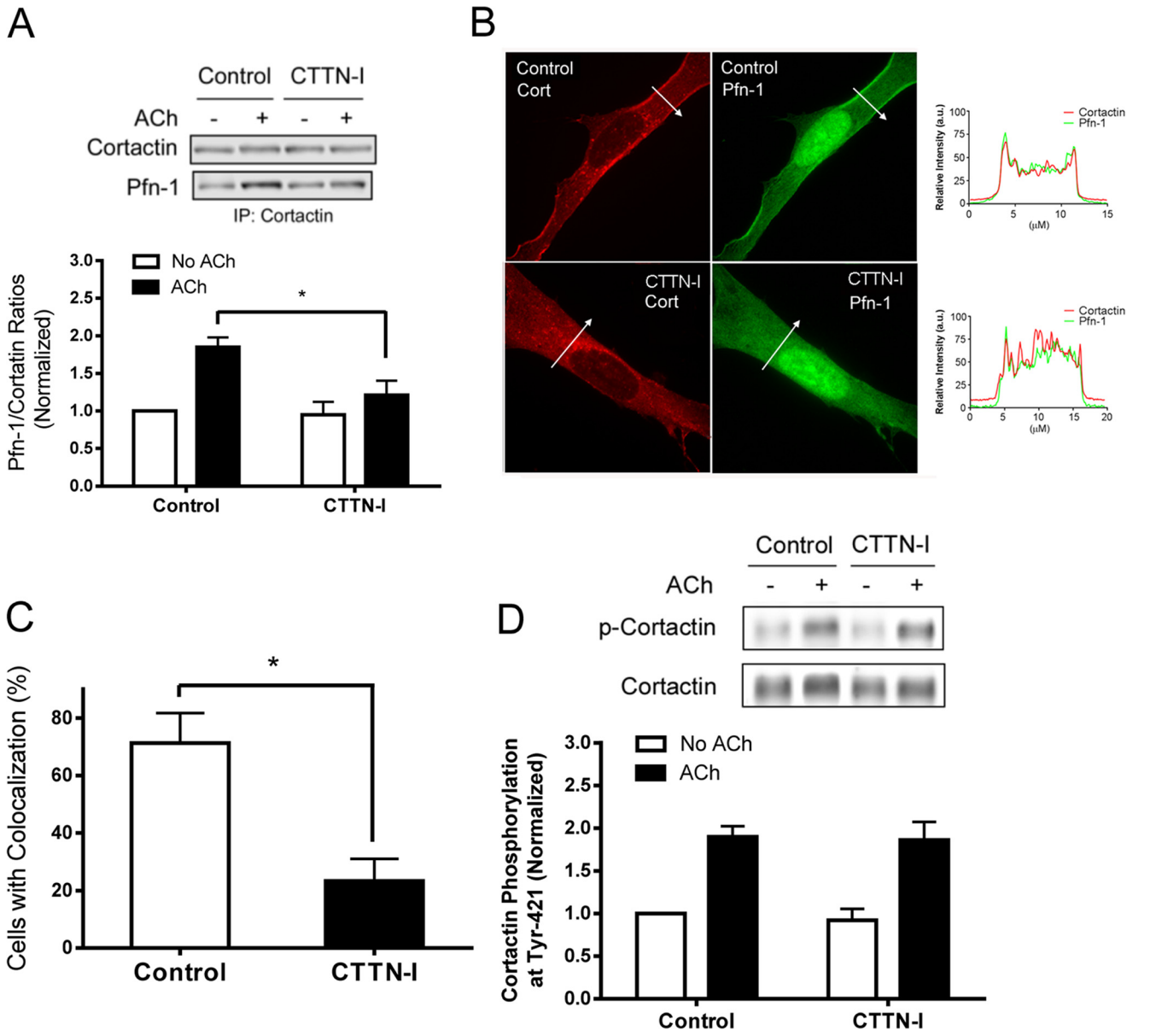


FIGURE 3. **Treatment with CTTN-I peptide inhibits cortactin/Pfn-1 coupling but not cortactin phosphorylation stimulated with ACh.** *A*, HASM cells were pretreated with control or CTTN-I peptide (2.5 $\mu$g/ml) for 20 min. Cells were then stimulated with ACh (100 $\mu$M; 5 min) or left unstimulated. The protein/protein interaction was evaluated by co-immunoprecipitation. Data are mean values of four independent experiments. *Error bars* indicate S.E. (*, $p < 0.05$). *B*, HASM cells pretreated with control or CTTN-I peptide were stimulated with ACh (100 $\mu$M; 5 min). The spatial localization of cortactin and Pfn-1 in the cells was assessed by immunostaining. *Arrows* indicate a single line scan to analyze the fluorescence signal for each cell. The line scan graphs show co-localization and relative fluorescence intensity of the two proteins. *Cort*, cortactin. *C*, the percentage of cells with colocalization was calculated as follows: (Number of cells with colocalization/Number of total cells observed) $\times$ 100. *, significantly different between cells treated with CTTN-I and cells treated with control peptide ($p < 0.05$; $n = 3$). *D*, HASM cells that had been pretreated with peptides were stimulated with ACh (100 $\mu$M; 5 min) or left unstimulated. Cortactin phosphorylation at Tyr-421 in these cells was evaluated. Cortactin phosphorylation is normalized to unstimulated cells treated with control peptide ($p > 0.05$; $n = 6$). *a.u.*, arbitrary units; *IP*, immunoprecipitation; *p-Cortactin*, phosphocortactin.

control tissues (Fig. 5*B*). Furthermore, cortactin knockdown reduced the ACh-induced F/G-actin ratios (Fig. 5*C*). However, myosin light chain phosphorylation at Ser-19 was not affected by cortactin silencing (Fig. 5*D*).

*Cortactin Undergoes Phosphorylation at Tyr-421 in HASM Cells during ACh Stimulation*—Cortactin undergoes tyrosine phosphorylation in nonmuscle cells (*e.g.* fibroblasts) during adhesion and migration (13, 14). To determine whether contractile stimulation induces cortactin phosphorylation, HASM cells were stimulated with ACh for different time periods or left unstimulated. Cortactin phosphorylation was evaluated by immunoblot analysis. Stimulation with ACh induced cortactin phosphorylation at Tyr-421 in smooth muscle cells. The phosphorylation levels of cortactin were increased as early as 1 min after ACh stimulation and sustained for 10 min after stimulation (Fig. 6*A*). Moreover, the ACh-induced cortactin phosphorylation was dose-dependent (Fig. 6*B*). We noticed that the increase in the average of the cortactin phosphorylation level did not plateau between $10^{-4}$ and $10^{-3}$ M ACh. This may be due to the relatively large variability of measurement between the two concentrations. In addition, m3 receptor is the predominant muscarinic subtype mediating

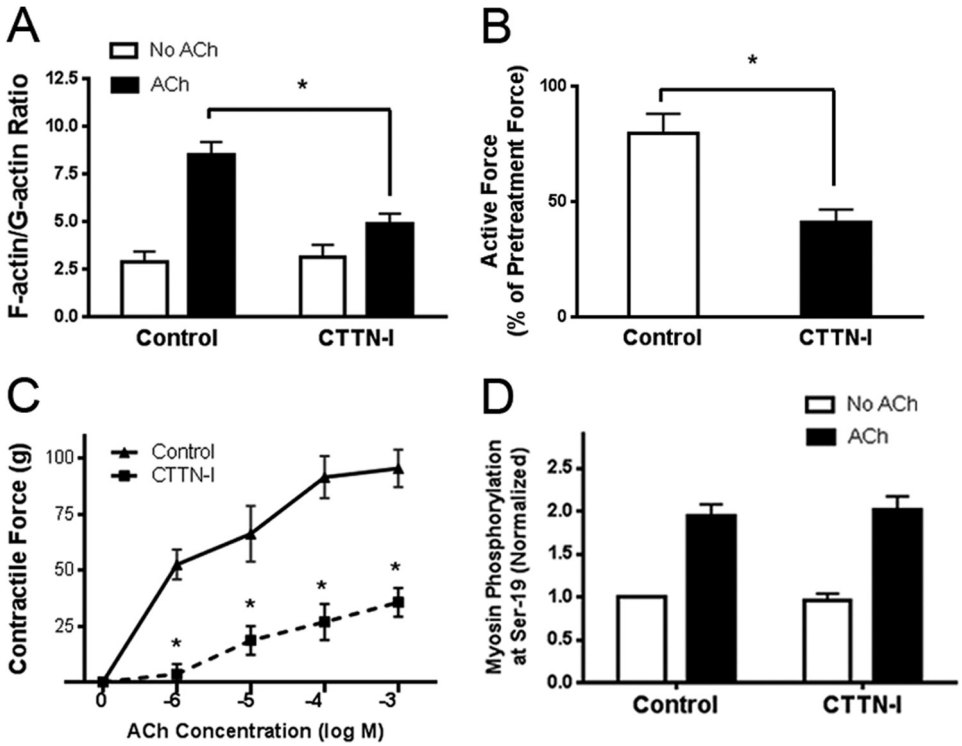


FIGURE 4. **Treatment with CTTN-I peptide attenuates increases in F/G-actin ratios and force development without affecting myosin phosphorylation.** *A*, HASM cells that had been pretreated with control or CTTN-I peptide were stimulated with ACh (100 $\mu$M; 5 min) or left unstimulated. F/G-actin ratios in cells were evaluated using the assay described under "Experimental Procedures." Data are mean values of six independent experiments. *Error bars* indicate S.E. (*, $p < 0.05$). *B*, contractile response of human bronchial rings to ACh was determined, after which they were pretreated with peptides (2.5 $\mu$g/ml) for 20 min. They were then stimulated with ACh. Contractile force is compared before and after the treatment with peptides (*, $p < 0.05$; $n = 3$). *C*, mouse tracheal segments were treated with peptides for 20 min. ACh dose response was then determined. *, significantly lower contractile force in CTTN-I peptide-treated segments than in control peptide-treated tissues at corresponding concentrations ($p < 0.01$; $n = 14$). *D*, myosin light chain phosphorylation in HASM cells pretreated with peptides was assessed by immunoblot analysis. Myosin phosphorylation was similar in cells pretreated with control peptide and in cells pretreated with CTTN-I peptide ($p > 0.05$; $n = 6$).

ACh-induced contractile response in airway smooth muscle (40).

*c-Abl Knockdown Inhibits Cortactin Phosphorylation in HASM Cells during Contractile Activation*—To identify the kinase that mediates cortactin phosphorylation in smooth muscle, we determined the effects of c-Abl KD on cortactin phosphorylation in smooth muscle because c-Abl is a tyrosine kinase that has a role in smooth muscle contraction (21, 23). c-Abl KD cells and cells expressing scrambled (control) shRNA were generated by lentivirus-mediated RNAi as described previously (16, 17). Immunoblot analysis verified the lower expression of c-Abl in c-Abl KD cells (Fig. 7*A*). Cortactin phosphorylation in control cells and c-Abl KD cells was evaluated by immunoblot analysis. The level of cortactin phosphorylation was higher in cells expressing control shRNA in response to ACh stimulation. However, ACh-induced cortactin phosphorylation was reduced in c-Abl KD cells. Cortactin phosphorylation in the absence of ACh was not different between cells producing control shRNA and c-Abl KD cells (Fig. 7*B*).

We also used an *in vitro* kinase assay to assess the role of c-Abl in cortactin phosphorylation. The phosphorylation level of cortactin was higher in the presence of c-Abl (Fig. 7*C*). The results suggest that cortactin phosphorylation is directly catalyzed by c-Abl.

*Interaction of Cortactin with Pfn-1 Is Inhibited by c-Abl KD*—To determine whether c-Abl has a role in regulating the association of cortactin with Pfn-1, stable c-Abl KD cells and cells expressing control shRNA were stimulated with ACh, or they were unstimulated. The interaction of cortactin with Pfn-1 was evaluated by co-immunoprecipitation analysis. In cells expressing control shRNA, the ratios of Pfn-1/cortactin during ACh stimulation were higher in stimulated cells as compared with unstimulated cells. In contrast, the ratios of Pfn-1/cortactin were reduced in c-Abl KD cells in response to ACh stimulation (Fig. 7*D*).

We have recently generated conditional knock-out (KO) mice in which c-Abl is disrupted in smooth muscle (c-Abl-KO mice) using cre-lox recombination (37). Conditional KO of c-Abl inhibits mouse tracheal ring contraction (37). We used co-immunoprecipitation analysis to assess the effects of c-Abl-KO on cortactin/Pfn-1 coupling. Treatment with ACh induced an increase in cortactin/Pfn-1 interaction in tracheal rings from c-Abl-flox mice. In contrast, the cortactin/Pfn-1 association was diminished in tracheal rings from c-Abl-KO mice during ACh stimulation (Fig. 7*E*).

*Cortactin Phosphorylation at Tyr-421 Affects Its Interaction with Pfn-1 during Contractile Activation*—Because contractile activation increases both cortactin phosphorylation and the association of cortactin with Pfn-1, it is possible that cortactin phosphorylation may modulate its interaction with Pfn-1. We used co-immunoprecipitation analysis to test this. In cells expressing wild type (WT) cortactin, stimulation with ACh increased the amount of Pfn-1 co-precipitated with cortactin. In contrast, the amount of Pfn-1 found in cortactin precipitates

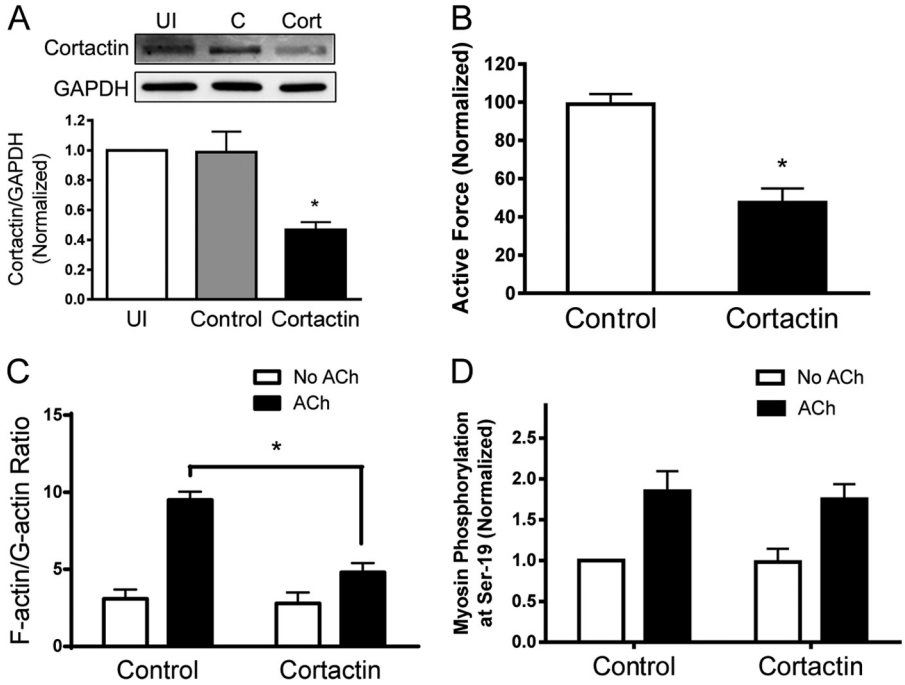


FIGURE 5. **Cortactin is required for airway smooth muscle contraction.** *A*, human bronchial rings were transduced with lentiviruses encoding control shRNA or cortactin shRNA. These tissues were then incubated in the serum-free medium for 3 days. Immunoblot analysis was used to assess the expression of cortactin in tissues. *UI*, uninfected; *C*, control shRNA; *Cort*, cortactin shRNA. *, significantly lower protein ratios of cortactin/GAPDH in tissues transduced with virus encoding cortactin shRNA than in uninfected tissues and tissues expressing control shRNA ($p < 0.05$). Data are mean values of three independent experiments. *Error bars* indicate S.E. *B*, contraction of human bronchial rings was evaluated, after which they were transduced with lentiviruses as described above. Contractile responses of tissues expressing cortactin shRNA were normalized to tissues expressing control shRNA. *, significantly lower contractile force in bronchial rings treated with cortactin shRNA as compared with tissues infected with virus encoding control shRNA ($p < 0.05$; $n = 3$). *C*, cells expressing control shRNA or cortactin shRNA were stimulated with ACh (100 $\mu$M; 5 min) or left unstimulated. F/G-actin ratios in cells were evaluated using the fractionation assay. Data are mean values of six independent experiments. *Error bars* indicate S.E. (*, $p < 0.05$). *D*, myosin light chain phosphorylation in HASM cells transduced with lentivirus encoding control or cortactin shRNA was assessed by immunoblot analysis. Myosin phosphorylation was similar in cells expressing control shRNA and cells expressing cortactin shRNA ($p > 0.05$; $n = 6$).

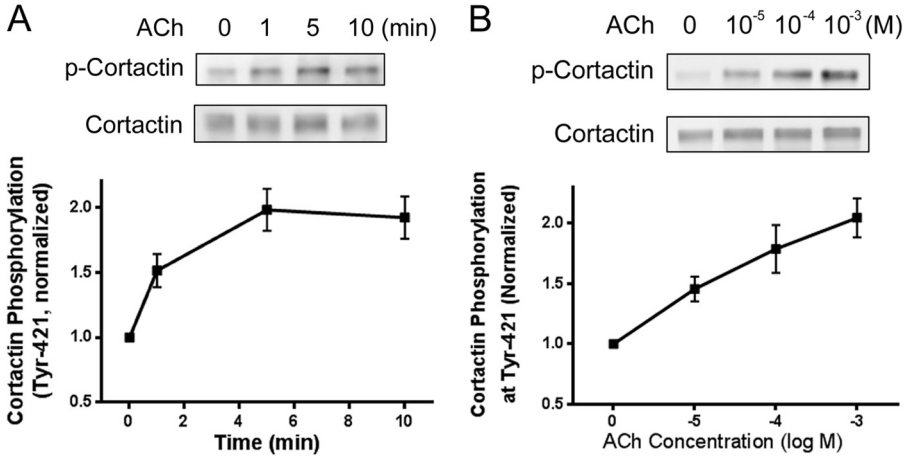


FIGURE 6. **Cortactin undergoes phosphorylation at Tyr-421 in cells in response to stimulation with ACh.** *A*, HASM cells were stimulated with 100 $\mu$M ACh for different time periods or left unstimulated. Cortactin phosphorylation in these cells was evaluated by immunoblot analysis. Cortactin phosphorylation upon ACh activation is time-dependent. Data are mean values of seven independent experiments. *Error bars* indicate S.E. *B*, cells were treated with different concentrations of ACh for 5 min. Cortactin phosphorylation was then assessed. ACh-induced cortactin phosphorylation at Tyr-421 is dose-dependent. Cortactin phosphorylation in cells induced by ACh is normalized to the levels in unstimulated cells ($n = 8$). *p-Cortactin*, phosphocortactin.

was reduced in cells expressing Y421F cortactin mutant upon ACh activation. Ratios of Pfn-1/cortactin during ACh stimulation were lower in cells expressing the mutant than in cells expressing WT cortactin (Fig. 7*F*).

*Knockdown of Abi1 Does Not Affect the Association of Cortactin with Pfn-1 upon Contractile Activation*—Our recent studies suggest that c-Abl regulates actin polymerization in part by regulating the activation of Abi1 (35). Because c-Abl is able to regulate cortactin/Pfn-1 coupling (Fig. 7, *D* and *E*), we questioned whether Abi1 is required for the protein/protein interaction by evaluating the effects of Abi1 KD on cortactin/Pfn-1 association. Immunoblot analysis verified Abi1 KD in these cells (Fig. 8*A*). Ratios of Pfn-1/cortactin were similar among uninfected cells, cells expressing control shRNA, and Abi1 KD

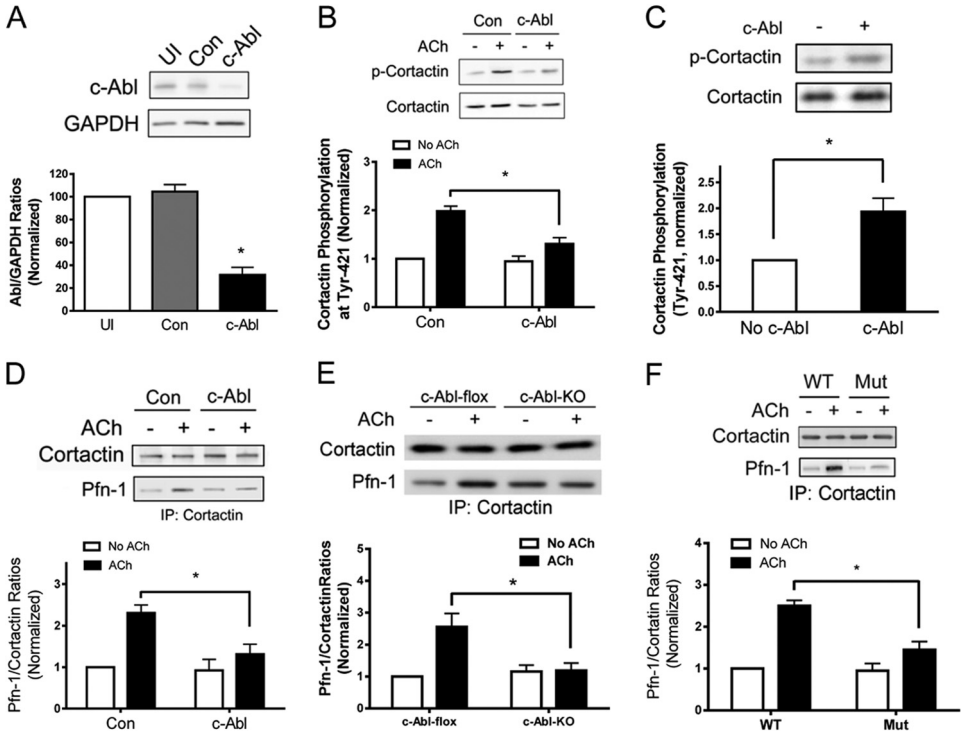


FIGURE 7. **c-Abl regulates cortactin phosphorylation and cortactin/Pfn-1 coupling in response to ACh stimulation.** *A*, silencing of c-Abl in HASM cells by lentivirus-mediated RNAi. Blots of extracts from uninfected (*UI*) cells and cells transduced with lentivirus encoding control (*Con*) shRNA or c-Abl shRNA were probed with antibodies against c-Abl and GAPDH. Protein ratios of c-Abl/GAPDH in cells expressing control or c-Abl shRNA are normalized to uninfected cells ($n = 6$). *, significantly lower c-Abl/GAPDH ratios in c-Abl KD cells than in uninfected cells and cells expressing control shRNA ($p < 0.05$). *B*, cells stably expressing control shRNA or c-Abl shRNA were stimulated with ACh (100 $\mu$M; 5 min) or left unstimulated. Cortactin phosphorylation of these cells was then evaluated. Cortactin phosphorylation is normalized to unstimulated cells expressing control shRNA. Data are mean values of five independent experiments. *Error bars* indicate S.E. (*, $p < 0.05$). *C*, cortactin phosphorylation by c-Abl *in vitro*. c-Abl-mediated cortactin phosphorylation was determined by *in vitro* kinase assay. Cortactin phosphorylation after c-Abl treatment is normalized to the phosphorylation level in the absence of c-Abl (*, $p < 0.05$; $n = 4$). *D*, control cells and c-Abl KD cells were stimulated with ACh (100 $\mu$M; 5 min), or they were unstimulated. Cortactin/Pfn-1 coupling was evaluated by co-immunoprecipitation ($n = 5$; *, $p < 0.05$). *E*, tracheal rings from c-Abl-flox mice or c-Abl-KO mice were treated with 100 $\mu$M ACh for 5 min or left untreated. Cortactin/Pfn-1 coupling was evaluated by co-immunoprecipitation analysis ($n = 4$; *, $p < 0.05$). *F*, cells expressing WT or mutant (Y421F) cortactin were stimulated with 100 $\mu$M ACh for 5 min or left unstimulated. Cortactin/Pfn-1 coupling was evaluated by co-immunoprecipitation analysis. Data are mean values of six independent experiments. *Error bars* indicate S.E. (*, $p < 0.05$). *IP*, immunoprecipitation; *p-Cortactin*, phosphocortactin; *Mut*, mutant.

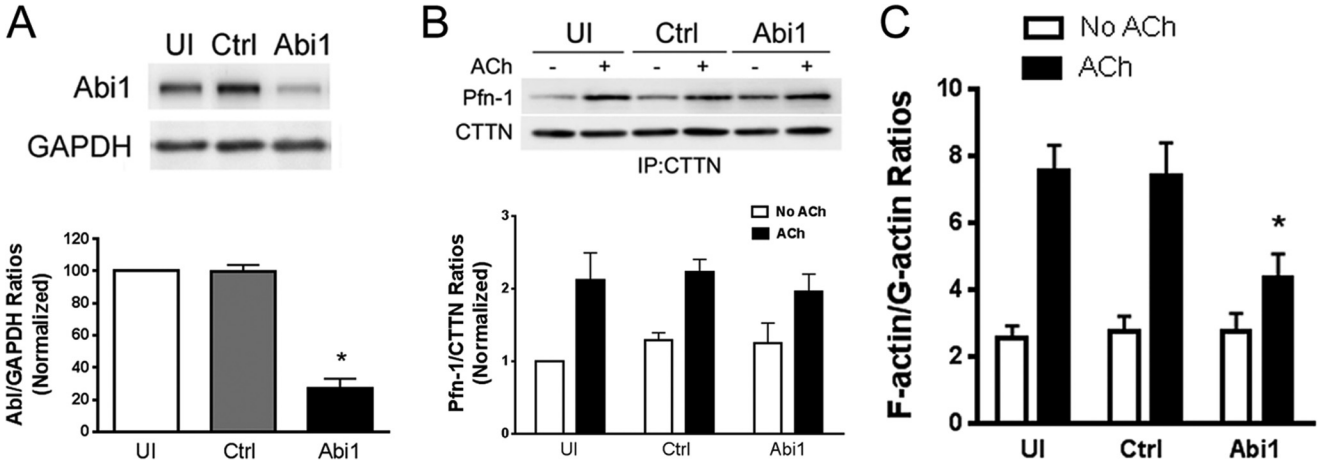


FIGURE 8. **Knockdown of Abi1 does not affect the association of cortactin with Pfn-1 upon ACh stimulation.** *A*, knockdown of Abi1 in cells by lentivirus-mediated RNAi. Blots of extracts from uninfected (*UI*) cells and cells transduced with lentivirus encoding control (*Ctrl*) shRNA or Abi1 shRNA were probed with antibodies against Abi1 and GAPDH. Abi1/GAPDH ratios in cells expressing control or Abi1 shRNA are normalized to uninfected cells ($n = 4$; *, $p < 0.05$). *B*, control cells and Abi1 KD cells were stimulated with ACh (100 $\mu$M; 5 min) or left unstimulated. Cortactin/Pfn-1 association was evaluated by co-immunoprecipitation. *CTTN*, cortactin. Data are mean values of four independent experiments. *Error bars* indicate S.E. ($n = 4$; $p > 0.05$). *C*, control cells and Abi1 KD cells were stimulated with ACh (100 $\mu$M; 5 min) or left unstimulated. F/G-actin ratios in cells were evaluated using the assay described under "Experimental Procedures" ($n = 5$; *, $p < 0.05$). *IP*, immunoprecipitation.

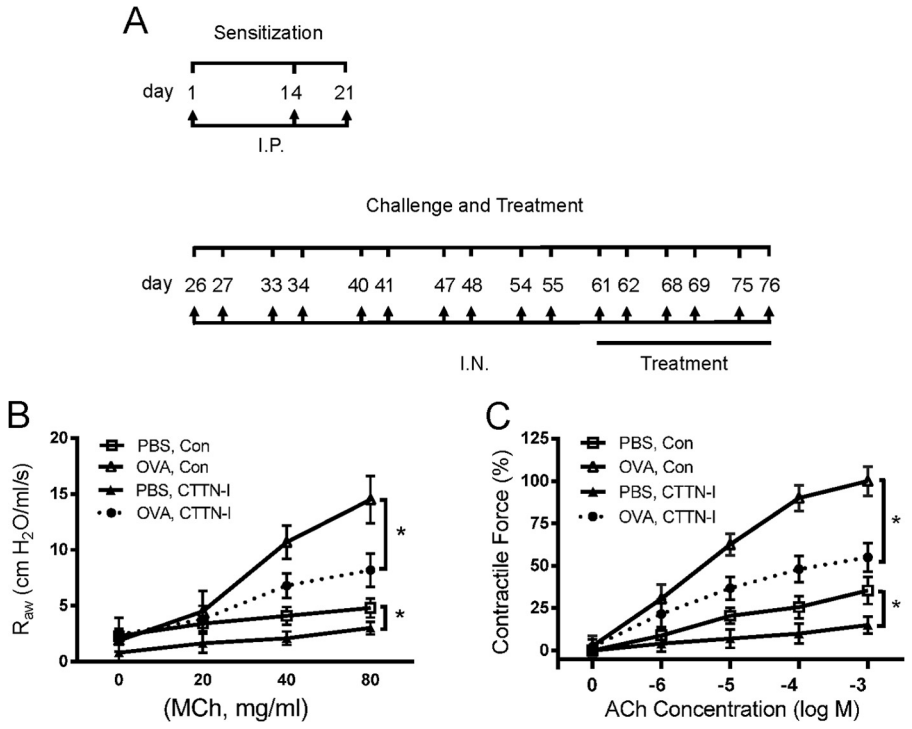


FIGURE 9. **Treatment with CTTN-I peptide diminishes airway resistance and contractile response of tracheal rings from OVA-sensitized and -challenged mice.** *A*, sensitization, challenge, and treatment protocol for the chronic asthma animal model. *I.P.*, intraperitoneal injection. *I.N.*, intranasal instillation. *B*, BALB/c mice were sensitized and challenged with OVA in the presence of control (*Con*) or CTTN-I peptide. Airway resistance ($R_{aw}$) in these mice was then measured. Intranasal instillation of CTTN-I peptide inhibits airway resistance in mice sensitized and challenged by OVA. Data are mean values of six independent experiments. *Error bars* indicate S.E. (*, $p < 0.05$). *C*, treatment with CTTN-I peptide attenuates OVA-sensitized tracheal contraction *ex vivo*. Contractile force is normalized to maximal force of rings from OVA- and vehicle-treated mice. Data are mean values of six independent experiments. *Error bars* indicate S.E. (*, $p < 0.05$). *MCh*, methacholine.

cells (Fig. 8*B*). However, actin polymerization upon ACh stimulation was affected by Abi1 KD (Fig. 8*C*). The results suggest that Abi1-regulated actin polymerization is not mediated by cortactin/Pfn-1 interaction during contractile stimulation.

*Inhibition of Airway Hyperresponsiveness and Airway Smooth Muscle Hypercontractility by CTTN-I Peptide*—Asthma is characterized by airway hyperresponsiveness, which is largely attributed to hyperreactivity of airway smooth muscle (41–44). However, the molecular mechanisms that control airway hyperresponsiveness and smooth muscle hyperreactivity are not fully understood. To determine whether the interaction of cortactin with Pfn-1 has a role in the process, we evaluated the effects of treatment with CTTN-I peptide on airway resistance in OVA-sensitized and -challenged BALB/c mice (Fig. 9*A*). Compared with mice treated with scrambled (control) peptide, airway resistance was lower in the OVA-sensitized and -challenged mice treated with CTTN-I peptide (Fig. 9*B*). Furthermore, the effects of CTTN-I peptide on contraction of isolated tracheal rings from the mice were assessed. The OVA-sensitized contractile force of isolated tracheal rings in response to ACh stimulation was lower in mice treated with CTTN-I peptide compared with animals treated with scrambled peptide (Fig. 9*C*).

## DISCUSSION

Actin dynamics plays a critical role in regulating smooth muscle contraction. Here, we unveil a novel mechanism that controls actin polymerization in smooth muscle. Contractile activation increases the association of cortactin with Pfn-1, which regulates actin dynamics and smooth muscle contraction. Furthermore, the interaction of cortactin with Pfn-1 is regulated by the c-Abl/cortactin pathway.

As described above, Pfn-1 is an actin-regulatory protein that is capable of modulating actin dynamics and force development in smooth muscle in response to contractile stimulation (7, 12, 45). However, the mechanisms that regulate Pfn-1 are not well understood. Here, contractile stimulation resulted in increases in the association of cortactin with Pfn-1 in smooth muscle. Moreover, disruption of this protein/protein interaction attenuated actin polymerization and force development without affecting myosin activation. Moreover, cortactin is necessary for actin dynamics and smooth muscle contraction. To the best of our knowledge, this is the first evidence to suggest that the interaction of cortactin with Pfn-1 is essential for the regulation of actin dynamics and smooth muscle contraction. The coupling of cortactin with Pfn-1 may promote the activation of Pfn-1, which in turn may facilitate actin dynamics and contraction in smooth muscle during agonist activation.

Cortactin activation may be regulated by Tyr-421 during migration of nonmuscle cells (14). Here, agonist activation induced phosphorylation of cortactin at Tyr-421 in smooth muscle, suggesting activation of cortactin in smooth muscle upon contractile stimulation. In nonmuscle cells such as mouse embryonic fibroblasts, cortactin phosphorylation is mediated by Src family kinases or Arg (13). c-Abl is a non-receptor tyro-

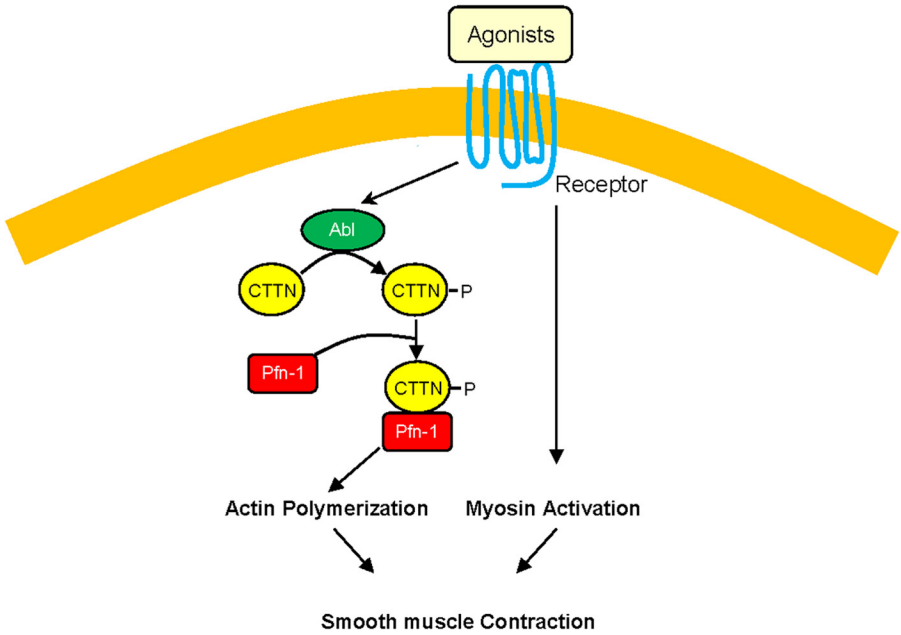


FIGURE 10. **Proposed mechanism for smooth muscle contraction.** In addition to myosin activation, contractile agonists may promote the association of cortactin (*CTTN*) with Pfn-1, which induces actin polymerization and smooth muscle contraction. The interaction of cortactin with Pfn-1 is regulated by cortactin phosphorylation and c-Abl tyrosine kinase.

sine kinase that has been implicated in smooth muscle contraction (21–23). In this study, knockdown of c-Abl attenuated the agonist-induced cortactin phosphorylation, demonstrating the important role of c-Abl in regulating cortactin phosphorylation in smooth muscle. Furthermore, cortactin can be phosphorylated by c-Abl *in vitro*, which is consistent with a previous study by others (28). It is likely that c-Abl may directly catalyze cortactin phosphorylation in smooth muscle in response to contractile activation.

Pfn-1 is able to interact with proline-rich domain-containing ligands such as palladin (39). The N-terminal and C-terminal helices of Pfn-1 form a binding cleft for poly-L-proline (26). It is likely that cortactin binds to Pfn-1 via the interaction of the proline-rich domain of cortactin with the cleft of Pfn-1. Structural analysis reveals that Tyr-421 is located in the proline-rich domain of cortactin (13, 14). In this study, cortactin Y421F mutant lost its affinity in smooth muscle cells upon contractile activation. These results suggest that the interaction of cortactin with Pfn-1 is regulated by phosphorylation at Tyr-421. Thus, Tyr-421 phosphorylation on cortactin may alter the conformation of the proline-rich domain and thus increase the association of cortactin with Pfn-1.

In this study, knockdown of c-Abl in smooth muscle attenuated the coupling of cortactin with Pfn-1 upon contractile activation. Furthermore, the agonist-induced actin polymerization and smooth muscle contraction were reduced in smooth muscle deficient of c-Abl. However, myosin light chain phosphorylation in smooth muscle during agonist activation was not affected by c-Abl silencing. Moreover, our recent studies suggest that c-Abl regulates actin polymerization in part by regulating the activation of Abi1 (35). In this study, knockdown of Abi1 attenuated actin dynamics without affecting cortactin/Pfn-1 coupling during contractile activation. Thus, c-Abl may have two important downstream cascades in smooth muscle. 1) c-Abl regulates cortactin phosphorylation, which subsequently regulates cortactin/Pfn-1 interaction, actin polymerization, and contraction. 2) c-Abl also controls the activation of the adapter protein Abi1, which in turn activates neuronal Wiskott-Aldrich syndrome protein, actin dynamics, and force development (35).

Actin polymerization may facilitate force development by several mechanisms. Actin polymerization may enhance the linkage of actin filaments to integrins, strengthening the transduction of mechanical force between contractile units and extracellular matrix (4, 7, 32, 33, 46, 47). In addition, actin filament assembly may also increase the numbers of contractile units and the length of actin filaments, providing more and efficient contractile elements for force development (48).

Allergic asthma is characterized by airway hyperresponsiveness, which largely stems from increased airway smooth muscle contraction (41). IL-13 has been implicated in the hyperactivity of airway smooth muscle (49). In addition, increases in intracellular $Ca^{2+}$ signaling may also contribute to the pathogenesis of smooth muscle hyperreactivity (50). In this study, we found that disruption of cortactin/Pfn-1 interaction by the peptide inhibited smooth muscle hypercontractility *ex vivo* and airway hyperresponsiveness *in vivo*. The results suggest that the association of cortactin with Pfn-1 is an important process that contributes to the development of airway hyperresponsiveness. Because c-Abl has been shown to mediate airway hyperresponsiveness (37), it is likely that c-Abl may induce airway hyperresponsiveness in part by modulating the coupling of cortactin with Pfn-1.

Here, we disclose a new cellular mechanism that regulates actin dynamics and contraction in smooth muscle. In addition to myosin activation, stimulation with contractile stimuli such as ACh promotes the association of cortactin with Pfn-1, which may activate Pfn-1, actin polymerization, and contraction. The

interaction of cortactin with Pfn-1 is modulated by the c-Abl/cortactin cascade (Fig. 10).

*Acknowledgment—We thank Olivia J. Gannon for technical assistance.*

## REFERENCES


1. Kamm, K. E., and Stull, J. T. (1989) Regulation of smooth muscle contractile elements by second messengers. *Annu. Rev. Physiol.* **51,** 299–313
2. Morgan, K. G. (2008) Contractility in health and disease. *J. Cell. Mol. Med.* **12,** 2157
3. Somlyo, A. V., Khromov, A. S., Webb, M. R., Ferenczi, M. A., Trentham, D. R., He, Z. H., Sheng, S., Shao, Z., and Somlyo, A. P. (2004) Smooth muscle myosin: regulation and properties. *Philos. Trans. R. Soc. Lond. B Biol. Sci.* **359,** 1921–1930
4. Gunst, S. J., and Zhang, W. (2008) Actin cytoskeletal dynamics in smooth muscle: a new paradigm for the regulation of smooth muscle contraction. *Am. J. Physiol. Cell Physiol.* **295,** C576–C587
5. Kim, H. R., Gallant, C., Leavis, P. C., Gunst, S. J., and Morgan, K. G. (2008) Cytoskeletal remodeling in differentiated vascular smooth muscle is actin isoform dependent and stimulus dependent. *Am. J. Physiol. Cell Physiol.* **295,** C768–C778
6. Rembold, C. M., Tejani, A. D., Ripley, M. L., and Han, S. (2007) Paxillin phosphorylation, actin polymerization, noise temperature, and the sustained phase of swine carotid artery contraction. *Am. J. Physiol. Cell Physiol.* **293,** C993–C1002
7. Tang, D. D., and Anfinogenova, Y. (2008) Physiologic properties and regulation of the actin cytoskeleton in vascular smooth muscle. *J. Cardiovasc. Pharmacol. Ther.* **13,** 130–140
8. Tang, D. D. (2009) p130 Crk-associated substrate (CAS) in vascular smooth muscle. *J. Cardiovasc. Pharmacol. Ther.* **14,** 89–98
9. Yang, C., Huang, M., DeBiasio, J., Pring, M., Joyce, M., Miki, H., Takenawa, T., and Zigmond, S. H. (2000) Profilin enhances Cdc42-induced nucleation of actin polymerization. *J. Cell Biol.* **150,** 1001–1012
10. Ding, Z., Lambrechts, A., Parepally, M., and Roy, P. (2006) Silencing profilin-1 inhibits endothelial cell proliferation, migration and cord morphogenesis. *J. Cell Sci.* **119,** 4127–4137
11. Fan, Y., Arif, A., Gong, Y., Jia, J., Eswarappa, S. M., Willard, B., Horowitz, A., Graham, L. M., Penn, M. S., and Fox, P. L. (2012) Stimulus-dependent phosphorylation of profilin-1 in angiogenesis. *Nat. Cell Biol.* **14,** 1046–1056
12. Tang, D. D., and Tan, J. (2003) Downregulation of profilin with antisense oligodeoxynucleotides inhibits force development during stimulation of smooth muscle. *Am. J. Physiol. Heart Circ. Physiol.* **285,** H1528–H1536
13. Ammer, A. G., and Weed, S. A. (2008) Cortactin branches out: roles in regulating protrusive actin dynamics. *Cell Motil. Cytoskeleton* **65,** 687–707
14. Cosen-Binker, L. I., and Kapus, A. (2006) Cortactin: the gray eminence of the cytoskeleton. *Physiology* **21,** 352–361
15. Lapetina, S., Mader, C. C., Machida, K., Mayer, B. J., and Koleske, A. J. (2009) Arg interacts with cortactin to promote adhesion-dependent cell edge protrusion. *J. Cell Biol.* **185,** 503–519
16. Wang, R., Mercaitis, O. P., Jia, L., Panettieri, R. A., and Tang, D. D. (2013) Raf-1, actin dynamics and Abl in human airway smooth muscle cells. *Am. J. Respir. Cell Mol. Biol.* **48,** 172–178
17. Jia, L., Wang, R., and Tang, D. D. (2012) Abl regulates smooth muscle cell proliferation by modulating actin dynamics and ERK1/2 activation. *Am. J. Physiol. Cell Physiol.* **302,** C1026–C1034
18. Qiu, Z., Cang, Y., and Goff, S. P. (2010) c-Abl tyrosine kinase regulates cardiac growth and development. *Proc. Natl. Acad. Sci. U.S.A.* **107,** 1136–1141
19. Hu, H., Bliss, J. M., Wang, Y., and Colicelli, J. (2005) RIN1 is an ABL tyrosine kinase activator and a regulator of epithelial-cell adhesion and migration. *Curr. Biol.* **15,** 815–823
20. Wang, J. Y. (2004) Controlling Abl: auto-inhibition and co-inhibition? *Nat. Cell Biol.* **6,** 3–7
21. Jia, L., and Tang, D. D. (2010) Abl activation regulates the dissociation of CAS from cytoskeletal vimentin by modulating CAS phosphorylation in smooth muscle. *Am. J. Physiol. Cell Physiol.* **299,** C630–C637
22. Chen, S., Wang, R., Li, Q. F., and Tang, D. D. (2009) Abl knockout differentially affects p130 Crk-associated substrate, vinculin, and paxillin in blood vessels of mice. *Am. J. Physiol. Heart Circ. Physiol.* **297,** H533–H539
23. Anfinogenova, Y., Wang, R., Li, Q. F., Spinelli, A. M., and Tang, D. D. (2007) Abl silencing inhibits CAS-Mediated process and constriction in resistance arteries. *Circ. Res.* **101,** 420–428
24. Li, Q. F., Spinelli, A. M., and Tang, D. D. (2009) Cdc42GAP, reactive oxygen species, and the vimentin network. *Am. J. Physiol. Cell Physiol.* **297,** C299–C309
25. Li, Q. F., Spinelli, A. M., Wang, R., Anfinogenova, Y., Singer, H. A., and Tang, D. D. (2006) Critical role of vimentin phosphorylation at Ser-56 by p21-activated kinase in vimentin cytoskeleton signaling. *J. Biol. Chem.* **281,** 34716–34724
26. Witke, W. (2004) The role of profilin complexes in cell motility and other cellular processes. *Trends Cell Biol.* **14,** 461–469
27. Brooks, H., Lebleu, B., and Vivès, E. (2005) Tat peptide-mediated cellular delivery: back to basics. *Adv. Drug Deliv. Rev.* **57,** 559–577
28. Boyle, S. N., Michaud, G. A., Schweitzer, B., Predki, P. F., and Koleske, A. J. (2007) A critical role for cortactin phosphorylation by Abl-family kinases in PDGF-induced dorsal-wave formation. *Curr. Biol.* **17,** 445–451
29. Pear, W. S., Nolan, G. P., Scott, M. L., and Baltimore, D. (1993) Production of high-titer helper-free retroviruses by transient transfection. *Proc. Natl. Acad. Sci. U.S.A.* **90,** 8392–8396
30. Wang, R., Li, Q. F., Anfinogenova, Y., and Tang, D. D. (2007) Dissociation of Crk-associated substrate from the vimentin network is regulated by p21-activated kinase on ACh activation of airway smooth muscle. *Am. J. Physiol. Lung Cell. Mol. Physiol.* **292,** L240–L248
31. Li, Q. F., and Tang, D. D. (2009) Role of p47(phox) in regulating Cdc42GAP, vimentin, and contraction in smooth muscle cells. *Am. J. Physiol. Cell Physiol.* **297,** C1424–C1433
32. Tang, D. D., Zhang, W., and Gunst, S. J. (2005) The adapter protein CrkII regulates neuronal Wiskott-Aldrich syndrome protein, actin polymerization, and tension development during contractile stimulation of smooth muscle. *J. Biol. Chem.* **280,** 23380–23389
33. Tang, D. D., and Gunst, S. J. (2004) The small GTPase Cdc42 regulates actin polymerization and tension development during contractile stimulation of smooth muscle. *J. Biol. Chem.* **279,** 51722–51728
34. Wang, R., Li, Q., and Tang, D. D. (2006) Role of vimentin in smooth muscle force development. *Am. J. Physiol. Cell Physiol.* **291,** C483–C489
35. Wang, T., Cleary, R. A., Wang, R., and Tang, D. D. (2013) Role of the adapter protein Abi1 in actin-associated signaling and smooth muscle contraction. *J. Biol. Chem.* **288,** 20713–20722
36. Wegmann, M., Göggel, R., Sel, S., Sel, S., Erb, K. J., Kalkbrenner, F., Renz, H., and Garn, H. (2007) Effects of a low-molecular-weight CCR-3 antagonist on chronic experimental asthma. *Am. J. Respir. Cell Mol. Biol.* **36,** 61–67
37. Cleary, R. A., Wang, R., Wang, T., and Tang, D. D. (2013) Role of Abl in airway hyperresponsiveness and airway remodeling. *Respir. Res.* **14,** 105
38. Coulson, F. R., and Fryer, A. D. (2003) Muscarinic acetylcholine receptors and airway diseases. *Pharmacol. Ther.* **98,** 59–69
39. Boukhelifa, M., Moza, M., Johansson, T., Rachlin, A., Parast, M., Huttelmaier, S., Roy, P., Jockusch, B. M., Carpen, O., Karlsson, R., and Otey, C. A. (2006) The proline-rich protein palladin is a binding partner for profilin. *FEBS J.* **273,** 26–33
40. Forsythe, S. M., Kogut, P. C., McConville, J. F., Fu, Y., McCauley, J. A., Halayko, A. J., Liu, H. W., Kao, A., Fernandes, D. J., Bellam, S., Fuchs, E., Sinha, S., Bell, G. I., Camoretti-Mercado, B., and Solway, J. (2002) Structure and transcription of the human m3 muscarinic receptor gene. *Am. J. Respir. Cell Mol. Biol.* **26,** 298–305
41. Amrani, Y., Tliba, O., Deshpande, D. A., Walseth, T. F., Kannan, M. S., and Panettieri, R. A., Jr. (2004) Bronchial hyperresponsiveness: insights into new signaling molecules. *Curr. Opin. Pharmacol.* **4,** 230–234
42. Guedes, A. G., Paulin, J., Rivero-Nava, L., Kita, H., Lund, F. E., and Kannan, M. S. (2006) CD38-deficient mice have reduced airway hyperresponsiveness following IL-13 challenge. *Am. J. Physiol. Lung Cell. Mol. Physiol.* **291,**

L1286–L1293
43. Ma, X., Cheng, Z., Kong, H., Wang, Y., Unruh, H., Stephens, N. L., and Laviolette, M. (2002) Changes in biophysical and biochemical properties of single bronchial smooth muscle cells from asthmatic subjects. *Am. J. Physiol. Lung Cell. Mol. Physiol.* **283,** L1181–L1189
44. Björck, T., Gustafsson, L. E., and Dahlén, S. E. (1992) Isolated bronchi from asthmatics are hyperresponsive to adenosine, which apparently acts indirectly by liberation of leukotrienes and histamine. *Am. Rev. Respir. Dis.* **145,** 1087–1091
45. Tang, D. D., and Tan, J. (2003) Role of Crk-associated substrate in the regulation of vascular smooth muscle contraction. *Hypertension* **42,** 858–863
46. Gunst, S. J., and Tang, D. D. (2000) The contractile apparatus and mechanical properties of airway smooth muscle. *Eur. Respir. J.* **15,** 600–616
47. Gerthoffer, W. T., and Gunst, S. J. (2001) Invited review: focal adhesion and small heat shock proteins in the regulation of actin remodeling and contractility in smooth muscle. *J. Appl. Physiol.* **91,** 963–972
48. Herrera, A. M., Martinez, E. C., and Seow, C. Y. (2004) Electron microscopic study of actin polymerization in airway smooth muscle. *Am. J. Physiol. Lung Cell. Mol. Physiol.* **286,** L1161–L1168
49. Tliba, O., Deshpande, D., Chen, H., Van Besien, C., Kannan, M., Panettieri, R. A., Jr., and Amrani, Y. (2003) IL-13 enhances agonist-evoked calcium signals and contractile responses in airway smooth muscle. *Br. J. Pharmacol.* **140,** 1159–1162
50. Deshpande, D. A., Dogan, S., Walseth, T. F., Miller, S. M., Amrani, Y., Panettieri, R. A., and Kannan, M. S. (2004) Modulation of calcium signaling by interleukin-13 in human airway smooth muscle: role of CD38/cyclic adenosine diphosphate ribose pathway. *Am. J. Respir. Cell Mol. Biol.* **31,** 36–42